Sensor Data Integrity: Final Report

ACFR, The University of Sydney

Prepared for:

Asian Office of Aerospace Research and Development (USA).

Report Documentation Page

Form Approved
OMB No. 0704-0188

1. REPORT DATE	2. REPORT TYPE	3. DATES COVERED
27 JAN 2009	**Final**	**13-05-2008 to 13-10-2008**

4. TITLE AND SUBTITLE	5a. CONTRACT NUMBER
Sensor Data Integrity	**FA48690814059**
	5b. GRANT NUMBER
	5c. PROGRAM ELEMENT NUMBER
6. AUTHOR(S)	5d. PROJECT NUMBER
Hugh Durrant-Whyte; Steven Scheding	5e. TASK NUMBER
	5f. WORK UNIT NUMBER
7. PERFORMING ORGANIZATION NAME(S) AND ADDRESS(ES)	8. PERFORMING ORGANIZATION REPORT NUMBER
University of Sydney,The University of Sydney J04,Sydney,Australia,NA,NSW 2006	**N/A**
9. SPONSORING/MONITORING AGENCY NAME(S) AND ADDRESS(ES)	10. SPONSOR/MONITOR'S ACRONYM(S)
AOARD, UNIT 45002, APO, AP, 96337-5002	**AOARD**
	11. SPONSOR/MONITOR'S REPORT NUMBER(S)
	AOARD-084059

12. DISTRIBUTION/AVAILABILITY STATEMENT

Approved for public release; distribution unlimited

13. SUPPLEMENTARY NOTES

14. ABSTRACT

This document constitutes the final report for the project ?Sensor Data Integrity? granted by the Asian Office of Aerospace Research and Development (USA). It describes the data that was collected for this work and proposes some preliminary elements of analysis. In particular, the documents enclosed present A presentation of the UGV System used to collect the data, including all sensors and calibration parameters A description of the data format and content A specification of all datasets provided separately A preliminary analysis of the performance of sensors depending on the environment conditions and of the search for sensor data integrity, with perspectives of work in this area.

15. SUBJECT TERMS

16. SECURITY CLASSIFICATION OF:			17. LIMITATION OF ABSTRACT	18. NUMBER OF PAGES	19a. NAME OF RESPONSIBLE PERSON
a. REPORT	b. ABSTRACT	c. THIS PAGE			
unclassified	**unclassified**	**unclassified**	**Same as Report (SAR)**	**53**	

Document Control Information

Document Owner: The point of contact for all questions regarding this document is

Project Leader:	Dr. Steven Scheding
Project Name:	Sensor Data Integrity
Phone:	+61 2 9351 8929
Fax:	+61 2 9351 7474
E-mail:	s.scheding@cas.edu.au

Document Creation: This document was created as follows

Creation Date:	2 December 2008
Created By:	Dr. Thierry Peynot

Document Identification: This document is identified as

File Name	Documents:ACFR:Projects:SensorDataIntegrity:FinalReport:SDIReport.pdf
Saved on:	03 December 2008, 11:52:00
Printed on:	10 December 2008, 14:04:00

Distribution Summary: This document is distributed to

Distribution:	Brian Skibba
Copy-to:	At discretion of Brian Skibba

Document Authorization: This revision of the current document is authorized for release in locked PDF form by

Authority Name: Olga Sawtell

Signed: _____ Date: _____

Revision History: The document revision history is listed with the most recent revision first.

Revision Date:
Version:
Revising Author(s):
Section(s) Revised:
Page No(s) Revised:
Summary of Changes:
Reviewed By:

Preface

Document Version Control: It is the Reader's responsibility to ensure that they have the latest version of this document. All questions should be directed to the Document Owner identified in the previous section of this document.

Privacy Information: This document contains information of a sensitive nature. It should not be transmitted in any form to individuals other than those involved in the project or those under express authorisation by the Project Leader.

Executive Summary

This document constitutes the final report for the project “Sensor Data Integrity” granted by the Asian Office of Aerospace Research and Development (USA).

It describes the data that was collected for this work and proposes some preliminary elements of analysis.

In particular, the documents enclosed present:

- A presentation of the UGV System used to collect the data, including all sensors and calibration parameters
- A description of the data format and content
- A specification of all datasets provided separately
- A preliminary analysis of the performance of sensors depending on the environment conditions and of the search for sensor data integrity, with perspectives of work in this area.

Sensor Data Integrity:
Final Report

Thierry Peynot, Sami Terho and Steven Scheding
ACFR, The University of Sydney

December 2008

Contents

List of Figures

Introduction

This project presents the first step towards developing and understanding integrity in perceptual systems for UGVs (Unmanned Ground Vehicles). Important issues addressed include;

- When do perceptual sensors fail, and why?
- What combination of sensors would be appropriate for a given operational scenario?
- Can perceptual sensor failure be reliably detected and mitigated?

Failure is a very broad term; it is hoped that through this work a UGV systems designer will have a better understanding of exactly what constitutes perceptual failure, how it may be designed for and its effects remediated. Such failures would not just include hardware failure, but also adverse environmental conditions (such as dust or rain), and algorithm failure.

To begin to address these issues, synchronised data have been gathered from a representative UGV platform using a wide variety of sensing modalities. These modalities were chosen to sample as much of the electromagnetic spectrum as possible, with the limitation that the sensors be feasible (and available) for use on UGVs. A preliminary analysis has then been performed on the data to ascertain the prime areas of competence of the sensors, and the combination of sensors most promising for a set of representative UGV scenarios.

Further work (not contained in this document) would develop the theoretical framework for sensor data-fusion and on-line integrity monitoring for use in UGV perceptual systems. In particular, the latter would provide an on-line "quality" evaluation of the environment perception and/or the environment modeling based on that perception [6], with sensor/modeling fault detection and isolation [5, 4]. This would constitute a susbtantial benefit for UGV navigation efficiency, robustness and safety.

This document is structured as follows: the first chapter presents the system used to gather the data, in particular the sensors involved (and their characteristics). The second chapter presents the datasets collected, listing the kind of environment, the conditions and the relevant information to be able to exploit the data. Finally, the third chapter gives a preliminary analysis of sensor data integrity, based on the gathered data.

Chapter 1

Presentation of the System

This chapter presents the system used to collect the data. It is composed of a ground vehicle called the Argo, equipped with various sensors.

1.1 The Argo vehicle

The vehicle used to collect the data, the CAS[1] Outdoor Research Demonstrator (CORD), is an 8 wheel skid-steering vehicle with no suspension (see figure 1.1), which turns thanks to pressure controlled brakes on both sides. It has a petrol engine, with a 12V alternator, and a 24V alternator to provide power to the computers and sensors on board.

Figure 1.1: The Argo Vehicle

For the purpose of this work, it has been equipped with multiple sensors, described in the following section.

[1]CAS stands for *Centre for Autonomous Systems*

1.2 The Sensors

All exteroceptive sensors are mounted on a sensor frame on top of the vehicle, as can be seen on figures 1.1 and 1.2.

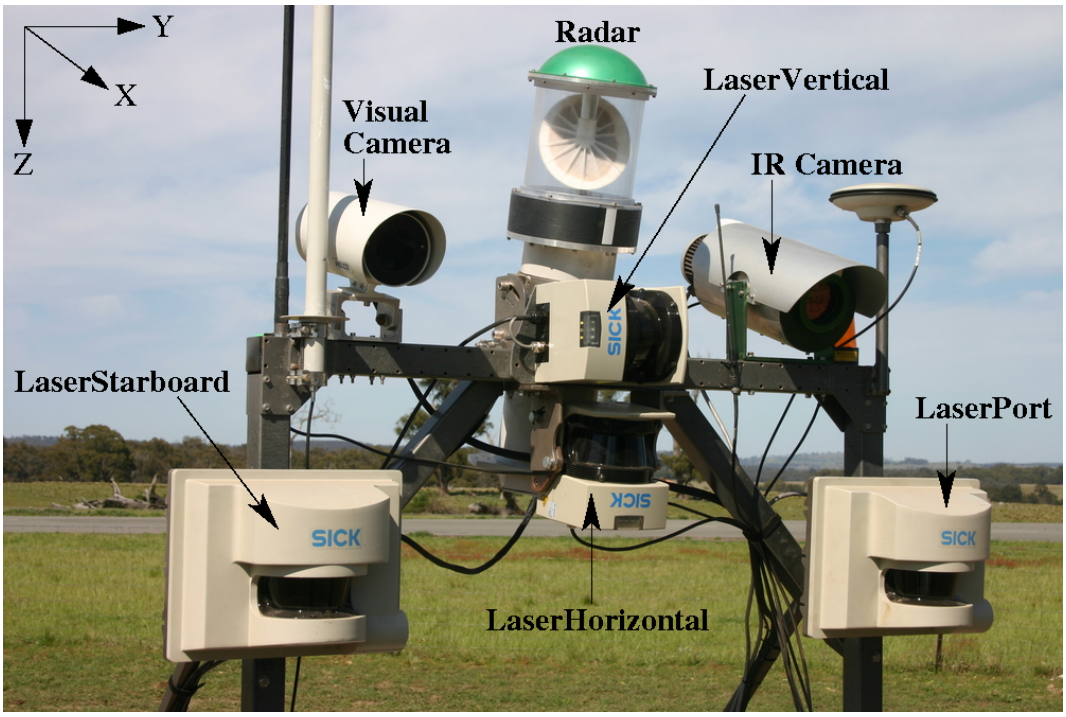

Figure 1.2: Argo Sensor Frame

1.2.1 Laser Range Scanners

Four laser range scanners are used. Two of them are SICK LMS 291, they are mounted at the center of the sensor frame. The two others are SICK LMS 221 mounted on both sides of that frame. The approximate configuration of these lasers, together with the names that will be used in the rest of this document, are the following[2] (see Figure 1.2. Note that *roll* corresponds to a rotation around axis X and *pitch* to a rotation around axis Y):

1. *LaserHorizontal*: centered on the sensor frame, slightly pointing down to the ground (a few degrees of pitch), zero roll[3].

2. *LaserVertical*: centered on the sensor frame, with 90 degrees roll (thus scanning vertically), zero pitch.

3. *LaserPort*: located on the Port side of the vehicle, this laser is slightly pointing down to the ground (a few degrees of pitch, less than for the *LaserHorizontal*), zero roll.

[2] see Section 1.2.5 on calibration for more precise estimation of their positions on the vehicle

[3] Note that this laser looks flipped over on fig. 1.2 (i.e. 180 deg. roll). However, this is accounted for in the process of data acquisition, thus it should be considered as with a zero roll.

4. *LaserStarboard*: located on the Starboard side of the vehicle, this laser is intended to have zero pitch and zero roll.

Characteristics and Nominal Performances

All four lasers were set to acquire data in the following mode:

- 0.25 degree resolution
- cm accuracy[4]
- 180 degree angular range[5]

1.2.2 FMCW Radar

This is a 94GHz Frequency Modulated Continuous Wave (FMCW) Radar (custom built at ACFR for environment imaging). Maximum rotation of scan head: 360 degrees at approximately 8Hz, 1KHz sample rate.

- Range resolution: $0.2m$.
- Maximum range: $40m$.

1.2.3 Visual Camera

The *Visual* camera (as opposed to the Infra-Red Camera) is a Prosilica Mono-CCD megapixel Gigabit Ethernet camera, pointing down (a few degrees of pitch).

Characteristics and Nominal Performances

- Image Pixel Dimensions: 1360×1024
- Resolution: 72×72 ppi (pixels per inch)
- RGB Colour, depth: 8 bits
- Nominal Framerate: 15 images per second in *static*[6] datasets, 10 images per second in *dynamic* datasets (unless specified differently).

1.2.4 Infra-Red Camera

Raytheon *Thermal-eye 2000B*. The images are acquired through a frame grabber providing digital images of size 640×480 pixels.

[4]except for the *cameras to lasers* calibration dataset, where the mm accuracy mode was used for more precision, but limiting the maximum range to 8m and the angular range to 100 degrees.

[5]except for the *cameras to lasers* calibration dataset, for which a 100 degree angular range was used.

[6]see section 3.2

Characteristics and Nominal Performances

- Image Pixel Dimensions of complete image: 640×480. In practice, though, the images are usually clipped to 511×398 to remove useless black bands on the sides. Actual sensor size: 320×240.
- Average Framerate: 12.5 images per second (unless specified differently).
- Spectral response range: $7 - 14\mu m$.

1.2.5 Calibration parameters

The spatial transformations between sensors and reference frames have been estimated using thorough calibration methods. The frames used are illustrated on Figure 1.3. They are named:

- *Navigation frame*: (fixed) global frame defined by the three axis: $X^n = North$, $Y^n = East$ and $Z^n = Down$ in which positions are expressed in UTM coordinates (Universal Transverse Mercator).
- *Body frame*: frame linked to the body of the vehicle, its centre being located at the centre of the IMU (Inertial Measurement Unit), approximately at the centre of the vehicle. The axis are: X^b pointing towards the from of the vehicle, Y^b pointing to the Starboard side of the vehicle, and Z^b pointing down.
- *Sensor frame*: frame linked to a particular sensor. It is defined in a similar way as the previous one (i.e. X^s forward, Y^s starboard, Z^s down), but centered on the sensor considered.

Note that in the rest of the document *Navigation* (or localisation) will correspond to the global positioning of the *Body frame* in the *Navigation frame*.

The *measured* distances between sensors are illustrated in figure 1.4. Note that an actual process of calibration usually provides better estimations of the real transformations between sensors. However these measured values are good initial estimates for calibration processes (and they were actually used as such in this work).

Two categories of calibration have been made:

- *Range Sensor Calibration*, to estimate the transformations between the frame associated to each range sensor (laser scanner or radar) and the *Body* frame.
- *Camera Calibration*, to estimate the intrinsic (geometric) parameters of each camera, and the extrinsic transformations between cameras and lasers.

Range Sensor Calibration

The estimation of the transformations between the frame associated to each range sensor (laser scanner or radar) and the Body frame was made using a technique detailed in [1, 8]. For that purpose, a dataset was acquired in an open area with flat ground and key geometric

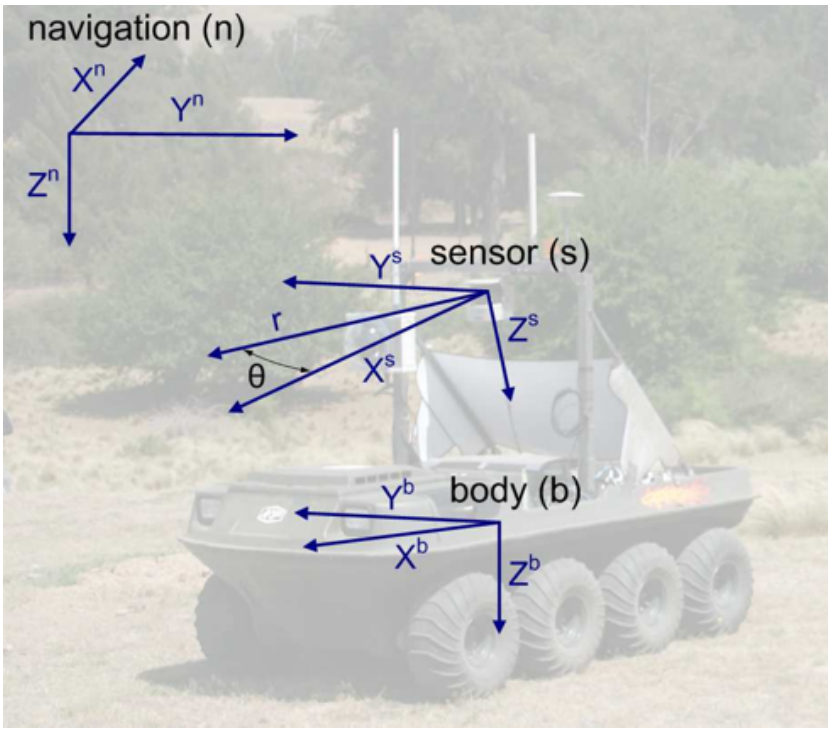

Figure 1.3: *Sensor*, *Body* and *Navigation* frames on the Argo

features such as a vertical metallic wall, two vertical poles with high reflectivity for lasers, and two vertical poles for the radar (see section 3.4.2).

The results of this calibration are the estimation of the 3 rotation angles ($RollX$, $PitchY$ and $YawZ$) and 3 translation offsets (dX, dY, dZ) from the Body frame to the Sensor frame. All angles will be expressed here in degrees for convenience and distances in metres.

The following table shows the results obtained after combined calibration of all four range sensors, i.e. *LaserHorizontal* (or *LaserH*), *LaserVertical* (or *LaserV*), *LaserPort* (or *LaserP*), *LaserStarboard* (or *LaserS*) and the *Radar*. Common features are used for all sensors. It is recommended to use these calibration results when combining the information from groups of these sensors.

Transformations Body Frame to Sensor Frame:

Sensor	RollX	PitchY	YawZ	dX	dY	dZ
LaserH	-0.732828	-8.586863	-1.631319	0.108987	0.008302	-0.919726
LaserV	88.562966	-0.118007	-1.123153	-0.000291	-0.082272	-1.126802
LaserP	-0.500234	-2.616210	-1.805911	0.190857	-0.548777	-0.763776
LaserS	-0.608178	-0.431051	-2.349991	0.198663	0.534253	-0.849538
Radar	-0.151571	191.161703	173.278081	-0.025753	-0.047174	-1.399104

Visual Camera Calibration

Intrinsic parameters The *intrinsic* calibration of each camera was made using the *Camera Calibration Toolbox for Matlab* [2].

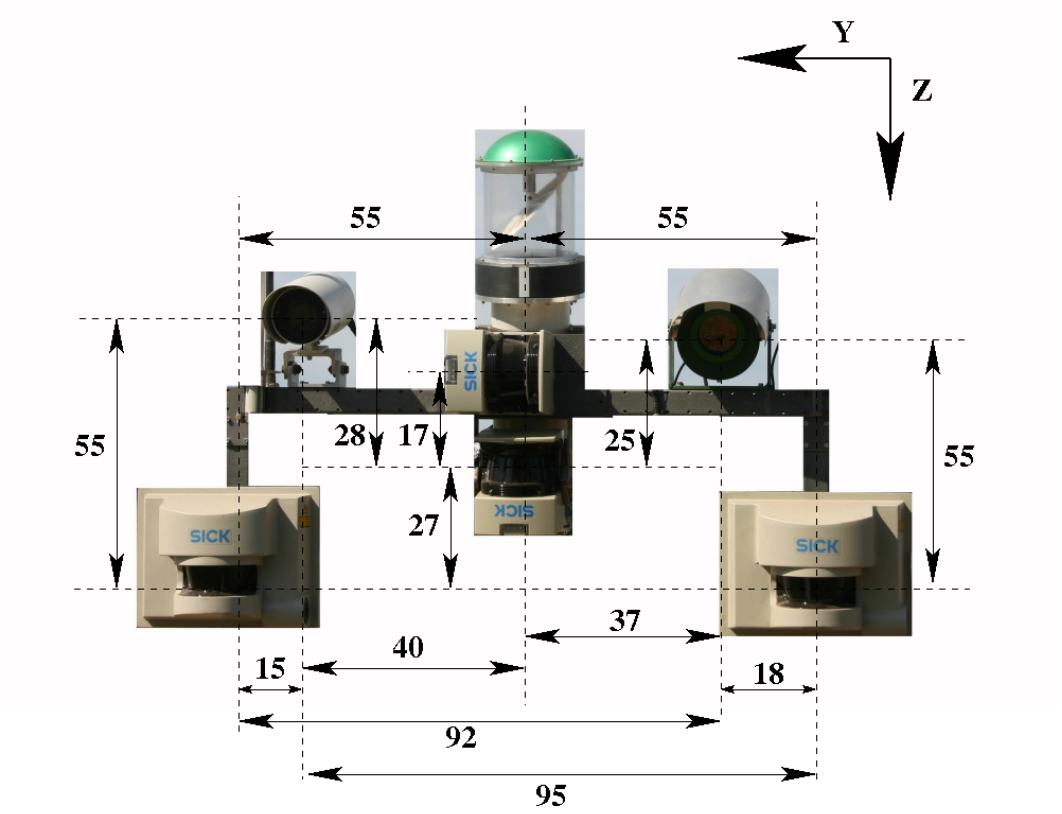

Figure 1.4: Distances between sensors in the (y, z) plane, in *cm*. Note that the dashed lines are meant to go through the centre of the sensors (despite any other impression due to perspective of the original picture).

The following is the content of the `Calib_Results.m` file exported by the toolbox, that describes the output of the calibration process in Matlab language:

```
%-- Focal length:
fc = [1023.094873083798120; 1020.891695892045050];
%-- Principal point:
cc = [643.139025535655492; 482.455417980580421];
%-- Skew coefficient:
alpha_c = 0.000000000000000;
%-- Distortion coefficients:
kc = [-0.218504818968279; 0.138951469767851;
      -0.000755791245166; 0.000175881419552; 0.000000000000000];
%-- Focal length uncertainty:
fc_error = [1.240637187529808; 1.220702756108720];
%-- Principal point uncertainty:
cc_error = [1.338561085455541; 1.362301725972313];
%-- Skew coefficient uncertainty:
alpha_c_error = 0.000000000000000;
%-- Distortion coefficients uncertainty:
kc_error = [0.001808042132202; 0.003689996468947;
      0.000207366100112; 0.000221355286767; 0.000000000000000];
%-- Image size:
nx = 1360;
ny = 1024;
```

The reader is invited to consult the toolbox web site [2] for more details on these parameters.

These output files from the calibration toolbox are included in the datasets.

Note that of the 93 images selected for the calibration process, 74 were actually used in the final optimisation process (see the file `Calib_Results.m` for details). The pixel error obtained for this calibration is:

```
Pixel error:  err = [ 0.19209 0.20252 ]
```

Extrinsic parameters (position of camera with respect to lasers) The extrinsic transformations between each camera and each laser was made using a method adapted from [7]. It uses the ouput of the Matlab Camera Calibration Toolbox to estimate the positions and orientations of the planes corresponding to the checker board visible in the images. These positions are compared with the positions of the laser points hitting this board. An optimisation process gives an estimation of the position of the laser range scanner with respect to the camera.

The following gives the three translations (δX_c, δY_c and δZ_c) and three rotations (ϕX_c, ϕY_c and ϕZ_c) enabling the placement of a point with original coordinates in the camera frame (using the convention used for the Matlab Toolbox: $+X_c$ to the right, $+Y_c$ down, $+Z_c$ forward) into the sensor frame linked to each laser. Distances are expressed in metres and angles in degrees.

***LaserHorizontal* to Visual camera:**

δX_c	δY_c	δZ_c	ϕX_c	ϕY_c	ϕZ_c
0.4139	-0.2976	-0.0099	-4.7341	-0.3780	-0.4230

***LaserVertical* to Visual camera:**[7]

δX_c	δY_c	δZ_c	ϕX_c	ϕY_c	ϕZ_c
0.5045	-0.0905	-0.208	-13.2030	-0.5851	-0.3140

***LaserPort* to Visual camera:**

δX_c	δY_c	δZ_c	ϕX_c	ϕY_c	ϕZ_c
0.9592	-0.5011	-0.0867	-10.6026	-0.0747	-0.5791

***LaserStarboard* to Visual camera:**

δX_c	δY_c	δZ_c	ϕX_c	ϕY_c	ϕZ_c
-0.1343	-0.4976	-0.0532	-12.6652	0.2409	-0.5293

IR Camera Calibration

Intrinsic parameters The intrinsic calibration of this camera was also made using the *Camera Calibration Toolbox for Matlab* [2].

The following is the content of the `Calib_Results.m` file exported by the toolbox, that describes the output of the calibration process in Matlab language:

```
%-- Focal length:
fc = [790.131547995049573; 826.825751328548790];
%-- Principal point:
cc = [328.685823692670340; 164.376489311973216];
%-- Skew coefficient:
alpha_c = 0.000000000000000;
%-- Distortion coefficients:
kc = [-0.466898225930376; 0.246094535921152;
      0.011203533644424; -0.005108186223306; 0.000000000000000];
%-- Focal length uncertainty:
fc_error = [5.782890597916310; 6.015102913624340];
%-- Principal point uncertainty:
cc_error = [9.426499879136482; 10.292926183444356];
%-- Skew coefficient uncertainty:
alpha_c_error = 0.000000000000000;
%-- Distortion coefficients uncertainty:
kc_error = [0.026759198529728; 0.152385380407985
      0.002604709115691; 0.002243445036632; 0.000000000000000];
%-- Image size:
nx = 640;
ny = 480;
```

Extrinsic parameters (position of cameras with respect to lasers) The same operations as for the visual camera were applied to determine the transformations between the IR camera frame and each laser.

[7] Note that this transformation was computed by combining the previous transformation *LaserHorizontal to camera* with the relative transformation of the two lasers found in the Range Sensor Calibration above, as the direct calibration method would not provide satisfying results.

***LaserHorizontal* to IR camera:**

δX_c	δY_c	δZ_c	ϕX_c	ϕY_c	ϕZ_c
-0.3391	-0.3278	0.0975	-6.5307	-1.2671	-2.1308

***LaserVertical* to IR camera:**[8]

δX_c	δY_c	δZ_c	ϕX_c	ϕY_c	ϕZ_c
-0.2485	-0.1207	-0.0115	-14.9996	-1.4742	-2.0218

***LaserPort* to IR camera:**

δX_c	δY_c	δZ_c	ϕX_c	ϕY_c	ϕZ_c
0.2090	-0.5400	0.0194	-12.7686	-1.0343	-2.3348

***LaserStarboard* to IR camera:**

δX_c	δY_c	δZ_c	ϕX_c	ϕY_c	ϕZ_c
-0.8772	-0.5652	0.0584	-15.7179	-0.8259	-3.3619

Note that the images and correspondings laser scans which were used for this calibration are available in the directory named `IRcameraCalibration` (see section 3.4.1). The images in this dataset are full resolution 640×480 as provided by the frame grabber, unlike the IR images in the other datasets which are clipped to keep only the part containing actual information.

1.2.6 Additional Sensors

Other sensors available on the Argo platform that will provide useful information are:

- Novatel SPAN System (Synchronized Position Attitude & Navigation) with a Honeywell IMU (Inertial Measurement Unit). This usually provides a 2cm RTK solution for localisation,
- Wheel encoders, measuring wheel angular velocities,
- Brakes sensors (position and pressure),
- Engine and gearbox rotation rate sensors.

[8] Note that this transformation was computed by combining the previous transformation *LaserHorizontal to camera* with the relative transformation of the two lasers found in the Range Sensor Calibration above.

Chapter 2

Data Format and Content

This chapter presents the format of the data provided. Section 2.1 describes the organisation of directories and files. Section 2.2 then precisely defines the format of the content of each file containing data. Note that in the rest of the document the Typewriter font will be used to designate names of `directories` or `files` and `text` written in ascii files.

2.1 Files and Directories Organisation

Each dataset has its directory containing all data from all sensors. It usually corresponds to a particular test (specific environment and conditions). Its name is composed of a number (corresponding to the chronological order of the data acquisition) and a string roughly describing the environment and conditions[1]. An example is: `04-StaticLightDust` for a *static*[2] test in the presence of light dust.

A dataset directory usually contains *eleven* sub-directories corresponding to the differents sensors involved (or type of data, see section 1.2); namely:

- `LaserHorizontal`
- `LaserPort`
- `LaserStarboard`
- `LaserVertical`
- `Nav`
- `Payload`
- `RadarRangeBearing`
- `RadarSpectrum`
- `VideoIR`
- `VideoVisual`

[1] a much more complete description is provided into each directory though

[2] See the more precise definition of *static* and *dynamic* test in chapter 3.

2.2 Ascii Log File Description

This section describes the content of the ascii files that can be found in each of the directories mentioned above.

Note that in all logged ascii files, the default units will be metres for all distances and radians for all angles (except for the Radar Spectrum data). Consequently, anywhere units are not clearly specified, metres and radians prevail. All files start with a time stamp, expressed in seconds, which corresponds to the *Unix* time.

Files contain one data sample (complete) message per line. The first columns of all ascii file have the general form:

```
*<timestamp> TEXT_TYPE data
```

where `TEXT_TYPE` is a string describing the type of data written on this line (e.g. `NAV_DATA` for navigation data) and `data` is the actual data from the sensor, written on as many columns as needed.

More specifically, the next sections describe the actual content of each type of file for each type of sensor or data. They will first indicate the name of the directory where the data can be found and then illustrate the content by a table.

2.2.1 Navigation (Localisation)

Name of directory: `Nav`.
The ascii data are contained in a file named `NavQAsciiData.txt`. The content of each line of this file is described in the following table. It corresponds to the global localisation of the vehicle (*Body frame*) expressed using the UTM coordinate system, in metres and radians.

Column:	1	2	3	4	5	6	7	8
Data :	`*<timestamp>`	`NAV_DATA`	North	East	Down	dNorth	dEast	dDown
Column:		9	10	11	12	13	14	15-158
Data:		RollX	PitchY	YawZ	dRoll	dPitch	dYaw	$C_{i,j}$

where $C_{i,j}$, $(i,j) \in [\![1,12]\!]^2$ are the elements of the covariance matrix describing the covariances between the 12 elements appearing in columns 3 to 14. Note that this matrix is written in rows: the whole row number 1 first, then row 2 etc... In other words, it is written as: $C_{1,1}, C_{1,2} \ldots, C_{1,12}, C_{2,1}, C_{2,2} \ldots C_{12,12}$.

2.2.2 Range Data from Lasers

This concerns the directories of the four lasers, namely:

- `LaserHorizontal`
- `LaserVertical`
- `LaserPort`
- `LaserStarboard`

In each of these directories, the ascii data are contained in a file named `RangeBearingQAsciiData.txt`. The content of each line of this file is described in the following table. Each line of the file typically shows the result of a 2D scan of 180 degrees with an increment of 1 degree. The first part of the line gives parameters describing this scan and the second part gives the actual range values returned by the laser sensor. 4 successive scans (i.e. 4 lines in the file), with starting angles each time incremented by 0.25 degree, will finally provide a full 180 degree wide and 0.25 degree resolution scan.

Column:	1	2	3	4
Data :	`*<timestamp>`	`RANGE_DATA`	`StartAngleRads`	`AngleIncrementRads`
Column:	5	6	7	$8 - end$
Data :	`EndAngleRads`	`RangeUnitType`	`NScans`	$\texttt{Range}_i$

where:

- `StartAngleRads` (*double*) is the value in radians of the first angle of the current scan (i.e. the one described on the current line of the file).
- `AngleIncrementRads` (*double*) is the difference of angle between two successive scan values (namely $\texttt{Range}_i$ and $\texttt{Range}_{i+1}$), in radians.
- `EndAngleRads` (*double*) is the value in radians of the last angle of the current scan (i.e. the current line).
- `RangeUnitType` is an integer showing the unit for the range values that follow in the line ($\texttt{Range}_i$). The possible integers and their meanings are as follow:
  - 1: mm
  - 2: cm
  - 3: m
  - 4: km
- `NScans` is the number N of scan values. Note that: $end = 8 + (\texttt{NScans} - 1)$
- $\texttt{Range}_i$ with $i \in [\![1, N]\!]$ are the actual range values for each angle of the current scan (the unit being determined by `RangeUnitTypeEnum`).

2.2.3 Radar Spectrum

The directory: `RadarSpectrum` contains the radar spectrum, described as the bins of a Fast Fourier Transform (FFT). The ascii data are contained in a file named `HSR_ScalarPoints1.txt`. The content of each line of this file is described in the following table:

Col.:	1	2	3 to end
Data:	`*<timestamp>`	`Angle`(degrees)	$\texttt{Reflectivity}_i$

where:

- `Angle` is the angle, in *degrees*, of the bins of this line.

- `Reflectivity`$_i$ with $i \in [\![1, N]\!]$ (N being the total number of bins on the line) are the reflectivity of each bin. Each of these bins correspond to a different range, with can be determined using the following.

First, note the following parameters, obtained after intrinsic calibration of the radar scanner:

- the Sample Frequency is $sampleFreq = 1250000Hz$.
- the frequency per metre is: $hertzPerM = 4336.384Hz/m$.
- the range offset is: $offsetM = -0.3507m$.

This means that the range associated to a particular bin (namely *binRange*) can be found by calculating:

$$\begin{array}{ll} frequencyHzPerBin & = sampleFreq/(2 * numberOfBins) \\ rangeMPerBin & = frequencyHzPerBin/hertzPerM \\ binRange & = bin \times rangeMPerBin + offsetM \end{array} \quad (2.1)$$

where *bin* represents the bin number (i.e. column number in the file - 2, starting with 1) and *binRange* is the range associated to this particular bin.

2.2.4 Range Data from Radar (RadarRangeBearing)

This concerns the directory named `RadarRangeBearing`. It contains range information from the radar, which is estimated from the spectrum. The ascii data are contained in a file named `RangeBearingQAsciiData.txt`. Its format is very similar to the laser files seen above, only with reflectivity information in addition to the range information. The content of each line of the file is described in the following table:

Col.:	1	2	3	4
Data:	`*<timestamp>`	`RANGE_REFLECTIVITY_DATA`	`StartAngleRads`	`AngleIncrRads`
Col.:	5	6	7	8
Data:	`EndAngleRads`	`RangeUnitType`	`NScans=1`	`Range`$_1$
Col.:	9			
Data:	`Reflectivity`$_1$			

where:

- `StartAngleRads` (double) is the value in radians of the first angle of the current scan (i.e. the one described on this line of the file).
- `AngleIncrRads` (double) is the difference of angle (increment) between two successive scan values. `AngleIncrRads` = 0 in this file, as there is only one range value per line.
- `EndAngleRads` (double) is the value in radians of the last angle of the current line. In practice, in this file, `EndAngleRads` = `AngleIncrRads`.
- `RangeUnitType` is an integer showing the unit for the range values that follow in the line. The possible integers and their meanings are as follow:
  - 1: mm

  - 2: cm
  - 3: m
  - 4: km

- `NScans` is the number of scan values. Here `NScans`=1 (one range value per line only).
- $\texttt{Range}_1$ is the actual range value for the current angle of the current scan (the unit being determined by the value of `RangeUnitTypeEnum`).
- $\texttt{Reflectivity}_1$ is the reflectivity of this current bin.

The range and reflectivity information contained in this file are extracted from the FFT (see section 2.2.3) by searching for the peak of highest reflectivity. The corresponding range that can be calculated by direct application of equation (2.1) is limited to the resolution of the discrete FFT: $0.28m$. Thus, to obtain a higher accuracy, a quadratic interpolation is performed on the peak processed from the signal: the interpolated range is the range obtained for the maximum point of the quadratic polynomial that is fitted to the three points of the FFT spectrum defining the peak (see [3] for more details).

2.2.5 *Internal* Data

Name of directory: `Payload`.
This concerns internal data from the vehicule, such as status of braking, wheel velocity etc... Note that this category of data is only relevant for the *dynamic* tests (moving vehicle). Thus they shall be found only in the directories of this category of datasets. The ascii data are contained in a file named `PayloadData1.txt`. The regular format of each line of this file is still:

```
*<timestamp> TEXT_TYPE data
```

with `TEXT_TYPE` having various possible values. These values and the corresponding line format and content of `data` are described in the table below. Note that, as previously, the first line of this table shows the column number.

1	2	3	4
*<timestamp>	SERVO_SETPOINT_DATA	chokePosition	throttlePosition
*<timestamp>	VELOCITY_TURN_RATE_DATA	velocity	turnRate
*<timestamp>	SENSOR_DATA	sensor	value
1	2	3	4
*<timestamp>	BRAKE_DATA	leftBrakePosition	rightBrakePosition
		5	6
		leftBrakePressure	rightBrakePressure
1	2	3	4
*<timestamp>	ACTUATOR_SETPOINT_DATA	desiredChoke	desiredThrottle
		5	6
		desiredLeftBrake	desiredRightBrake

When `TEXT_TYPE` = `SENSOR_DATA`, `sensor` is an integer referring to a particular internal sensor. The possibilities and the corresponding meaning for `value` are illustrated in the following

table:

sensor	value (unit)
0	Engine Rotation Rate (RPM)
1	Gearbox Rotation Rate (RPM)
2	12V Battery Voltage (V)
3	24V Battery Voltage (V)
4	Left Wheel Angular Velocity (rad/s)
5	Right Wheel Angular Velocity (rad/s)

Note that these data are provided for information, but a model of the vehicle would be needed to actually make the BRAKE_DATA, ACTUATOR_SETPOINT_DATA and the RPM information really useful for the reader. It is recommended to contact the authors in that case.

2.2.6 Camera Images

Two directories concern camera images: one for the Infra-Red Camera (**VideoIR**) and one for the Visual Camera (**VideoVisual**). Both contain the same kind of data:

- One ascii file named VideoLogAscii.txt, with the following format:

Column:	1	2	3
Data:	*<timestamp>	VISION_FRAME	<filename>

- One directory Images containing all the bmp images (as files) provided by the camera. Those files have the names described in the VideoLogAscii.txt file. Note that this name is formed by the prefix 'Image' followed by a timestamp (where the '.' between seconds and fractions of seconds has been replaced by a '-'), plus the extension '.bmp'.

Chapter 3

Data sets

There are two types of datasets. In the *static* ones the vehicle is stationary and the sensors acquire data always from the same area. The area contains: features with known characteristics and dimensions inside an identified frame, and objects and equipment used for creating the environmental conditions (e.g. a compressor and a water pump), outside of the frame. In the *dynamic* datasets the vehicle moves around the test area, which usually contains the same equipment as mentioned before, plus a car (from which the UGV was operated).

The purpose of the static datasets was to acquire data in different conditions but with the same features, to enable a comparison of the effects of different environmental conditions.

Note that *static* or *dynamic* will refer to the state of the vehicle, not the status of the environment, which can be considered as static except if the presence of a moving element such as a *human* is present.

The beginning and ending times of the datasets are expressed in three formats. The first column shows the Unix time, that is, seconds after midnight UTC of January 1, 1970. The leap seconds are not counted in this convention. The second column shows the UTC time. UTC stands for Universal Timing Convention, and is equivalent to the Greenwich Meridian Time (GMT). The third column shows the local AEDT time in the test site. AEDT stands for: Australian Eastern Daylight Saving Time.

As the data acquisition was made with several (synchronised) computers, sensor data logging does not necessarily start at the exact same time for all sensors. Thus, for convenience, the **Start** and **End** time correspond respectively to the earliest and the latest time of the dataset when all data from all sensors are available.

The next section describes each type of conditions that appear in the datasets.

3.1 Environmental conditions

The simulated environmental conditions include dusty environment, smoke, rain, and clear environment without any adverse environmental conditions.

3.1.1 Dust

The dust was generated by blowing air to dusty soil. The blower was a high-power air compressor with a flexible tube for directing the air. Some of the datasets were gathered in areas where the soil was naturally very dusty. In these cases the dust was generated by

blowing the air to the ground near the vehicle. In the other cases the dusty soil was collected and piled near the actual test site, and the air was blown to the pile to generate a cloud of dust.

3.1.2 Smoke

Orange smoke was generated with smoke bombs that worked for about one minute. The bomb was held by an assistant, choosing their position so that the wind carried the smoke towards the vehicle. Sometimes the direction of the wind varied, so the assistant would move to compensate.

3.1.3 Rain in static environment

In the static tests the rain was generated with sprinklers attached to the top of a frame defining the test area (see figure 3.2). This frame covered an area being 9.3 meters long and 4.3 meters wide. The water was stored in a tank equipped with a pump to bring the water to the sprinkler system. This device is visible on the right side of the frame and the vehicle.

3.1.4 Rain in dynamic environment

In the dynamic tests the rain was generated with the same tank as in the static tests, but instead of sprinklers, the rain was simulated by spraying the water with a hand-held hose pointed at the vehicle's working area.

3.2 Static tests

In the static tests the vehicle was standing still and imaging an area with known features, inside the sprinkler frame used for generating the rain. These objects were generally chosen to be easily detected by the sensors in clear conditions. Most of them are artificial and of simple geometry (e.g. box or pole) and their dimensions are provided: figure 3.1 shows a drawing of this area with location of the features. However, a branch of tree (attached to a metal bar stuck into the ground) was also set in the test area to have a natural feature. The elements of figure 3.1 are also listed in the table 3.1 for more details. The positions of these features were chosen so that every sensor (in particular the 2D laser scanners) can see at least some of them and the objects are distributed over the area.

The framerate of the visual camera in this series of tests was 15 frames per second, except in the first dataset where the framerate was 10 frames per second.

The vehicle was facing south. Therefore the sun was either behind or on the side of the vehicle. As the data sets were collected in Australia, sun shines from the north in the middle of the day. Note that in this section, features mentioned will be located with respect to the vehicle, i.e. *left* will refer to the *Port* side if the Argo, while *right* will refer to its *Starboard* side.

3.2.1 Day 1: Afternoon and evening

The first set of static trials data was acquired on the 15th of October 2008, in the afternoon and in the evening. Most of the datasets were acquired when the sun was above the horizon, except for one, acquired just after sunset. The wind was quite strong, and it affected significantly

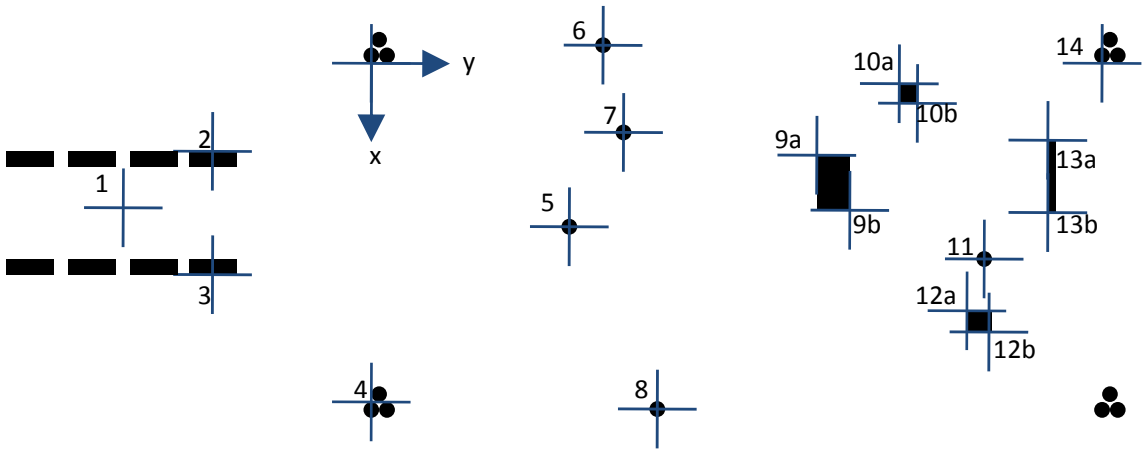

Figure 3.1: Static trial setup seen from above

	Object name	**X (cm)**	**Y (cm)**	**Diam. (cm)**	**Height (cm)**	
origin	Supporting pole of the frame on the left side of Argo	0	0			
1	Centre of Argo sensor frame	190	-293		185	
2	Port front wheel of Argo	112	-202			
3	Starboard front wheel of Argo	269	-202			
4	Supporting pole of the frame on the right side of the Argo	431	0			
5	Tree	108	252	5		(1)
6	Laser pole	-23	295		175	
7	Radar reflector on the top of a pole	88	321		114	(2) **(3)**
8	Laser pole	440	364		175	
9	Two plastic boxes on top of each other: First box	117...187	567...609		33	
	Second plastic box	117...147	578...598		33...67	
10	Brick tower	26...51	672...695		100	
11	Radar reflector on the ground	249	780		29	**(3)**
12	Canister	315...342	758...786		45	
13	Table standing on its side	98...190	861		122	
14	Supporting pole of the frame on the left back side	0	930			

(1) The branch is at the height of 90cm. The foliage of the tree reaches about 120cm to the right.
(2) The radar reflector is hanging so that the top of it is on the top of the supporting pole.
(3) Note that these radar reflectors are present in the test area **only for datasets number 24 to 26**.

Table 3.1: Elements present in the static trial setup

Figure 3.2: Photo of the static trial area (Datasets 01 to 24)

dust and smoke spreading. The wind was mainly blowing from the left with respect to the vehicle.

01-02 - Clear conditions

The first two datasets were acquired in clear conditions, without any artificially created dust, smoke or rain. In the first dataset the frame rate of the color camera was 10 frames per second, and in the second one the frame rate was 15 frames per second.

Dataset name: 01-StaticClear-Video10fps

	Unix	UTC	AEDT
Start	1224050945.437	06:09:05.437	15:09:05.437
End	1224051090.447	06:11:30.447	15:11:30.447
Duration	145.010 seconds		

Dataset name: 02-StaticClear-Video15fps

	Unix	UTC	AEDT
Start	1224051487.381	06:18:07.381	15:18:07.381
End	1224051619.116	06:20:19.116	15:20:19.116
Duration	131.735 seconds		

03 - Clear conditions with human

This dataset was acquired in clear conditions. A human (intentionally) is walking through the area.

Dataset name: 03-StaticClear-Human

	Unix	UTC	AEDT
Start	1224052418.386	06:33:38.386	17:33:38.386
End	1224052519.662	06:35:20.662	17:35:20.662
Duration	101.276 seconds		

04 - Light dust

In this dataset, an assistant blew dust from a pile that was located on the left, out of the test area. The dust was carried by wind from left to right with respect to the sensors. The dust cloud mainly occurred between the sensors and the test area. The dust density was relatively low. The dataset started and ended in clear conditions.

Dataset name: 04-StaticLightDust

	Unix	UTC	AEDT
Start	1224053469.229	06:51:09.229	17:51:09.229
End	1224053602.855	06:53:23.855	17:53:23.855
Duration	133.626 seconds		

Figure 3.3: Human walking in the test area during a static test (Dataset 03)

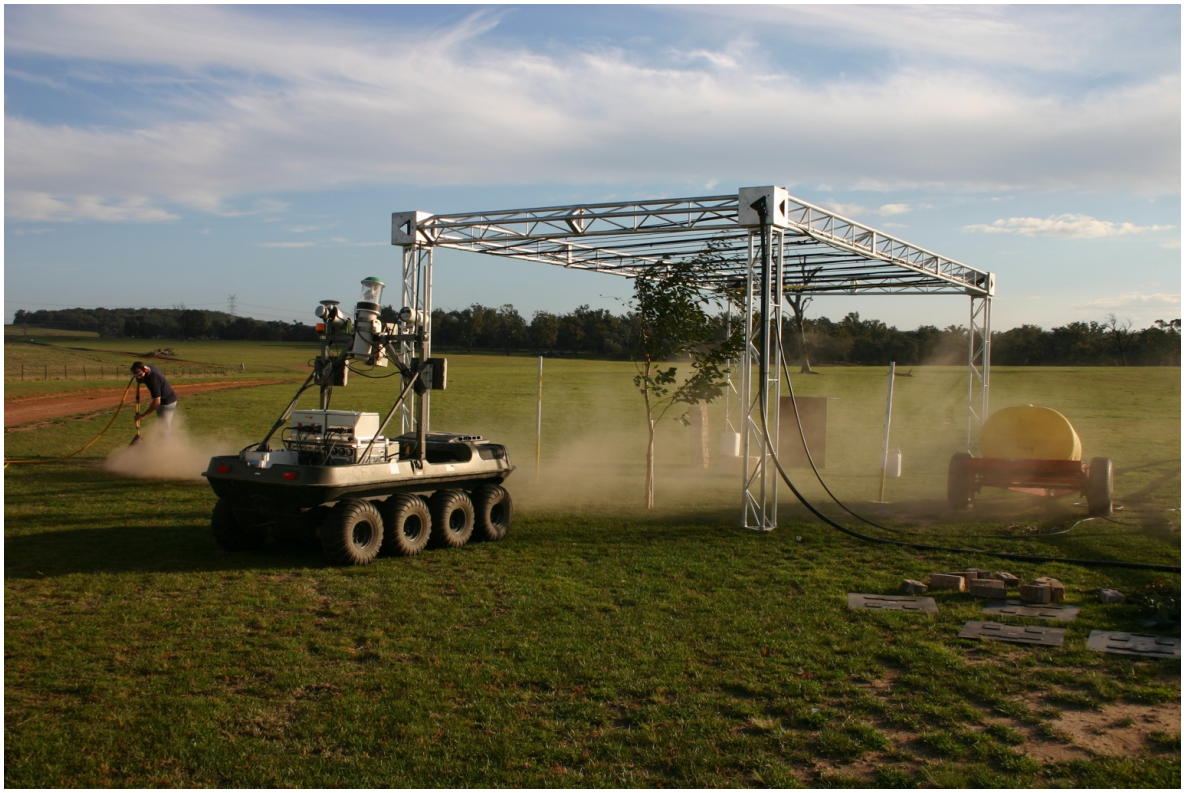

Figure 3.4: Static test with light dust (Dataset 04)

05 - Heavy dust

As previously, in this dataset an assistant blew dust from a pile that was located on the left, out of the test area. The dust was carried by the wind from left to right with respect to the sensors, and it moved between the sensors and the test area. The dust cloud was denser than before. The dataset started and ended in clear conditions.
Note that the lasers and radar data start 14 to 18 seconds later than the other sensors.

Dataset name: 05-StaticHeavyDust

	Unix	UTC	AEDT
Start	1224054044.006	07:00:44.006	18:00:44.006
End	1224054110.171	07:01:50.171	18:01:50.171
Duration	66.165 seconds		

06 - Light dust with human

As in the two previous cases, an assistant blew dust from a pile that was located on the left of the test area. The dust was carried by wind from left to right. The dust cloud mainly occurred between the sensors and the test area. The dust density was relatively low. A human was walking around the test area. The dataset started and ended in clear conditions.

Dataset name: 06-StaticLightDust-Human

	Unix	UTC	AEDT
Start	1224055857.924	07:30:58.924	18:30:58.924
End	1224055992.320	07:33:12.320	18:33:12.320
Duration	134.396 seconds		

07 - Smoke

An assistant held a smoke bomb in the left of the test area. The smoke moved almost entirely between the sensors and the test area. The dataset started and ended in clear conditions.

Dataset name: 07-StaticSmoke

	Unix	UTC	AEDT
Start	1224056457.502	07:40:58.502	18:40:58.502
End	1224056543.290	07:42:23.290	18:42:23.290
Duration	85.788 seconds		

08 - Heavy rain

The sprinklers were used to create heavy rain. Wind from the left biased the rain towards the right, and therefore the left part of the test area had less rain than the right part. Rain was present during the whole dataset.

Dataset name: 08-StaticHeavyRain

	Unix	UTC	AEDT
Start	1224056989.625	07:49:50.625	18:49:50.625
End	1224057123.862	07:52:04.862	18:52:04.862
Duration	134.237 seconds		

Figure 3.5: Static test with smoke(Dataset 07)

09 - Heavy rain with human

As before, the sprinklers were used to create heavy rain. A human was walking around the test area. Wind from the left biased the rain towards right again. Rain was present during the whole dataset.

Dataset name: 09-StaticHeavyRain-Human

	Unix	UTC	AEDT
Start	1224057199.911	07:53:20.911	18:53:20.911
End	1224057280.261	07:54:40.261	18:54:40.261
Duration	80.350 seconds		

10 - Light rain

The sprinklers were used to create lighter rain. As in the previous cases, wind from the left biased the rain towards right with respect to the sensors. The rain was created during the whole dataset.

Dataset name: 10-StaticLightRain

	Unix	UTC	AEDT
Start	1224057494.661	07:58:15.661	18:58:15.661
End	1224057652.537	08:00:53.537	19:00:53.537
Duration	157.876 seconds		

11 - Clear conditions after rain

This dataset was acquired right after the rain datasets, with the sprinklers turned off. Consequently, all the objects in the test area were wet, and a few drops of water were occasionally still falling from the top of the frame. The sun was very low but still above the horizon during the acquisition of this dataset.

Dataset name: 11-StaticAfterRainEvening

	Unix	UTC	AEDT
Start	1224057998.295	08:06:38.295	19:06:38.295
End	1224058157.685	08:09:18.685	19:09:18.685
Duration	159.390 seconds		

12 - Clear conditions after rain and sunset

This dataset was acquired just after sunset. There is still reasonable light, but the sun is already below the horizon. This dataset was acquired shortly after the rain datasets as well, so all the objects in the test area were still wet, with also the possibility of having a few drops of water still falling. Note that the lasers data logs stop about 88 seconds before the rest of the data.

Dataset name: 12-StaticClearAfterRainAfterSunset

	Unix	UTC	AEDT
Start	1224058839.207	08:20:39.207	19:20:39.207
End	1224058972.002	08:22:52.002	19:22:52.002
Duration	132.795 seconds		

3.2.2 Day 2: Morning and midday

The second set of static trials was realized on the 16th of October 2008, starting in the morning and lasting until midday. In all of the datasets sun was high in the sky. There was much less wind than during the first day, and its direction varied.

14 - Clear

This dataset was acquired in clear conditions, without any artificially created dust, smoke or rain.

Dataset name: 14-StaticMorningClear

	Unix	UTC	AEDT
Start	1224112428.048	23:13:48.048	10:13:48.048
End	1224112600.636	23:16:41.636	10:16:41.636
Duration	172.588 seconds		

15 - Heavy dust

An assistant blew dust from a pile that was located west of the test area. The dust was carried by wind from left to right with respect to the sensors. The dust cloud moved a bit to south-east, and therefore the north-eastern corner of the area was not completely covered with dust. The dust density was high. The dataset started and ended in clear conditions. The Figure 3.6 shows the dust cloud.

Dataset name: 15-StaticMorningHeavyDust

	Unix	UTC	AEDT
Start	1224113347.161	23:29:07.161	10:29:07.161
End	1224113448.576	23:30:49.576	10:30:49.576
Duration	101.415 seconds		

16 - Very light dust

An assistant blew dust from a dusty road west of the test area. Part of the dust was carried by wind from left to right with respect to the sensors. The dust cloud was very thin when it reached the test area. The dataset started and ended in clear conditions.

Dataset name: 16-StaticMorningVeryLightDust

	Unix	UTC	AEDT
Start	1224114064.835	23:41:05.835	10:41:05.835
End	1224114139.801	23:42:20.801	10:42:20.801
Duration	74.966 seconds		

17 - Smoke

An assistant held a smoke bomb that generated smoke to the test area. The wind was very weak, but strong enough to carry the smoke towards the test area. The direction of the wind changed during the test. The assistant was first standing at the left side of the test area, then

Figure 3.6: Static test with heavy dust (Dataset 15)

Figure 3.7: Static test with smoke (Dataset 17)

he moved to the back of it and finally to the right side. The assistant was always standing outside of the test area. The dataset started and ended in clear conditions with no smoke.

Dataset name: 17-StaticMorningSmoke

	Unix	UTC	AEDT
Start	1224114471.313	23:47:51.313	10:47:51.313
End	1224114571.005	23:49:31.005	10:49:31.005
Duration	99.692 seconds		

18 - Light rain

The sprinklers were used to create light rain. The weak wind did not affect much the direction of the rain. Note that the area closer to the sensors did not get as much rain as the area further away. Besides, the rain was not completely uniform in the area, due to a leak in the front.

Dataset name: 18-StaticMorningLightRain

	Unix	UTC	AEDT
Start	1224117868.591	00:44:29.591	11:44:29.591
End	1224117989.562	00:46:30.562	11:46:30.562
Duration	120.971 seconds		

19 - Rain

The sprinklers were used to create heavier rain. The weak wind did not affect much the direction of the rain.

Dataset name: 19-StaticMorningRain

	Unix	UTC	AEDT
Start	1224120580.504	01:29:41.504	12:29:41.504
End	1224120739.598	01:32:20.598	12:32:20.598
Duration	159.094 seconds		

20 - Smoke

An assistant held a smoke bomb that generated smoke to the test area. In this test the direction of the wind did not change much. The assistant was mainly standing at the back-right corner of the test area. The assistant's arm may have entered the test area in the beginning. The dataset started and ended in clear conditions with no smoke. As this dataset was acquired after the rain, all the objects were wet.

Dataset name: 20-StaticMorningSmoke

	Unix	UTC	AEDT
Start	1224120901.096	01:35:01.096	12:35:01.096
End	1224120989.101	01:36:29.101	12:36:29.101
Duration	88.005 seconds		

21 - Clear conditions after rain and smoke

This dataset was acquired after the smoke and rain datasets. All the objects in the test area were wet, and there might be some residue from the smoke.

Dataset name: 21-StaticMorningClearAfterRainAndSmoke

	Unix	UTC	AEDT
Start	1224121144.696	01:39:05.696	12:39:05.696
End	1224121263.788	01:41:04.788	12:41:04.788
Duration	119.092 seconds		

3.2.3 Day 2: Morning and midday - with added radar reflectors

The second part of the second day's tests was done in the same area, but with two additional features in the area: radar reflectors. Also their positions are marked in the figure 3.1. The figure 3.9 shows the test area with the radar reflectors.

22 - Clear

The reflectors are still in the test area. The dataset was acquired in clear conditions.

Figure 3.8: Static test with smoke (Dataset 20)

Figure 3.9: Static test area with radar reflectors (Datasets 22 & 23)

Dataset name: 22-StaticMorningClearWithReflectors

	Unix	UTC	AEDT
Start	1224122292.159	01:58:12.159	12:58:12.159
End	1224122430.871	02:00:31.871	13:00:31.871
Duration	138.712 seconds		

23 - Clear, human walking

In this dataset the human was walking around the test area. The human did not interact especially with the radar reflectors but walked past them.

Dataset name: 23-StaticMorningClearWithReflectors-Human

	Unix	UTC	AEDT
Start	1224122579.975	02:03:00.975	13:03:00.975
End	1224122682.009	02:04:42.009	13:04:42.009
Duration	102.034 seconds		

24 - Clear, human walking near reflectors

In this dataset the human was also walking around the test area. Unlike for the previous dataset, the walking pattern was related to the radar reflectors. The human walked near the radar reflectors, first behind the reflector, then between the reflector and the sensors, and finally, on the side of the reflector. This was repeated for both reflectors.

Dataset name: 24-StaticMorningClearWithReflectors-HumanNearReflectors

	Unix	UTC	AEDT
Start	1224122950.838	02:09:11.838	13:09:11.838
End	1224123096.280	02:11:36.280	13:11:36.280
Duration	145.442 seconds		

3.2.4 Summary of *Static* Datasets

The following table summarizes the conditions for each of these datasets taken with *static* vehicle.

Dataset	Dust	Smoke	Rain	Human	Comment
01-02					Clear
03				X	
04-05	X				
06	X			X	
07		X			
08			X		
09			X	X	
10			X		
11					Clear, evening
12					Clear, after sunset
14					Clear, morning
15-16	X				
17		X			
18 & 19			X		
20		X			
21					
22					with radar reflectors
23-24				X	with radar reflectors

3.3 Dynamic tests

In the dynamic tests, the vehicle was driving around different areas and acquiring data from the environment. Simulated environmental conditions such as dust, rain and smoke, were also created for some datasets. Unlike for the static datasets, the rain was produced with mobile equipment.

3.3.1 Open area

The tests in this section were realized in an open area, on mostly flat ground. The soil on the ground is very dusty, which means that rapid movements of the vehicle produce thick clouds of dust without any external input. On the northern side of the area is a shed with metal walls. Next to the shed, there is a fence. Another fence is located on the south-western side of the area. Both fences consist of barbed wire and wooden posts. The area is bounded by an unpaved road on the eastern side. Figure 3.10 shows an aerial image of the area. This test area is on the left side of the image. Figure 3.11 shows a photo of the area.

29 - Clear conditions during day

This dataset was acquired during daytime. The vehicle was driving around the area avoiding sharp turns that would have caused much dust.

Dataset name: 29-DynamicDayTriangleClear

	Unix	UTC	AEDT
Start	1224198733.114	23:12:13.114	10:12:13.114
End	1224199111.326	23:18:31.326	10:18:31.326
Duration	378.212 seconds		

Figure 3.10: Aerial image of the *open area* (on the left side of the path) and the *houses area* (on the right side of the path)

Figure 3.11: Photo of the *open area* (Datasets 25 to 32)

Figure 3.12: Dynamic test in the open area with dust (Datasets 30 & 31)

30-31 - Dust during day

These datasets were acquired during daytime. The vehicle was driving around the area while an assistant produced the dust. The ground of the area is very dusty, so the dust was produced just by pointing the blower to the ground. The assistant needed to walk around the test area. They can be seen in the dataset.

Dataset name: 30-DynamicDayTriangleDust

	Unix	UTC	AEDT
Start	1224199788.106	23:29:48.106	10:29:48.106
End	1224199986.155	23:33:06.155	10:33:06.155
Duration	198.049 seconds		

Dataset name: 31-DynamicDayTriangleMoreDust

	Unix	UTC	AEDT
Start	1224200313.353	23:38:33.353	10:38:33.353
End	1224200500.152	23:41:40.152	10:41:40.152
Duration	186.799 seconds		

32 - Clear conditions after dust on day

This dataset was acquired after the datasets with dust. The objects in the area are probably more dusty than in the earlier dataset in clear conditions.

Dataset name: 32-DynamicDayTriangleClearAfterDust

	Unix	UTC	AEDT
Start	1224201093.019	23:51:33.019	10:51:33.019
End	1224201271.635	23:54:32.635	10:54:32.635
Duration	178.616 seconds		

25-27 - Clear conditions at night with external lights on

These datasets were acquired at nighttime. The sun had set completely, so all the light was artificially created. A car was parked in the test area. The headlights of the car were on and pointing towards the area where the test vehicle moved. The vehicle's own headlights also illuminated the area in front of it. Note that in dataset 27 the door of the shed was open with the internal light of the building on. This can be seen in the images of the camera.

Dataset name: 25-DynamicNightClearTriangleWithCarLights

	Unix	UTC	AEDT
Start	1224158167.214	11:56:07.214	22:56:07.214
End	1224158524.566	12:02:05.566	23:02:05.566
Duration	357.352 seconds		

Dataset name: 27-DynamicNightClearTriangleWithCarLights2

	Unix	UTC	AEDT
Start	1224159874.355	12:24:34.355	23:24:34.355
End	1224160153.568	12:29:14.568	23:29:14.568
Duration	279.213 seconds		

26-28 - Clear conditions at night without external lights

These datasets were acquired at nighttime, the only artificial light coming from the vehicle's own headlights.

Dataset name: 26-DynamicNightClearTriangleNoCarLights

	Unix	UTC	AEDT
Start	1224158859.005	12:07:39.005	23:07:39.005
End	1224159161.470	12:12:41.470	23:12:41.470
Duration	302.465 seconds		

Dataset name: 28-DynamicNightClearTriangleNoCarLights2

	Unix	UTC	AEDT
Start	1224160333.789	12:32:14.789	23:32:14.789
End	1224160606.918	12:36:47.918	23:36:47.918
Duration	273.129 seconds		

Summary

The following table summarizes the conditions for each of these datasets taken in the *open area*.

Dataset	Dust	Daytime	Night w. Ext. Light	Night no Ext. Light	Comment
29		X			Clear
30-31	X	X			
32		X			After dust
25 & 27			X		Ext. car lights
26 & 28				X	

3.3.2 Area with houses

This is an area with three wooden buildings. A long building is standing in the southern side of the area. Two smaller ones are on the northern side. The area is bounded by a fence. This area can be seen on the right side of the aerial image in figure 3.10.

33 - Clear conditions without humans

This dataset was acquired in the daytime. The vehicle was driving around the area with houses (see figure 3.13).

Dataset name: 33-DynamicDayHousesClear

	Unix	UTC	AEDT
Start	1224201950.093	00:05:50.093	11:05:50.093
End	1224202213.225	00:10:13.225	11:10:13.225
Duration	263.132 seconds		

34 - Clear conditions, human walking around

This dataset was acquired at daytime. The vehicle was driving around the same area as before and in similar conditions. However, in addition to the previous dataset, a human was walking around during the test.

Dataset name: 34-DynamicDayHouses-Human

	Unix	UTC	AEDT
Start	1224202880.040	00:21:20.040	11:21:20.040
End	1224203087.626	00:24:48.626	11:24:48.626
Duration	207.586 seconds		

3.3.3 Area with trees and water

This is an area next to a lake. On the southern side of the area there is a small eucalyptus forest. A photo of the area is shown in figure 3.14.

35 - Clear conditions

This dataset was acquired at daytime. The vehicle was driving around the area.

Figure 3.13: Dynamic test around the houses (Datasets 33 & 34)

Figure 3.14: Photo of the area with trees and a lake (Datasets 35 to 40)

Dataset name: 35-DynamicDayDamClear

	Unix	UTC	AEDT
Start	1224216067.282	04:01:07.282	15:01:07.282
End	1224216412.990	04:06:53.990	15:06:53.990
Duration	345.708 seconds		

36-37 - Dust

These datasets were acquired during daytime. An assistant produced the dust by pointing the blower to the ground. It was not as dusty as in the open area, and therefore there was less dust in this area. The assistant had to move a little in order to create the dust in front of the vehicle. The figure 3.15 shows a photo of the actual situation.

Dataset name: 36-DynamicDayDamDust

	Unix	UTC	AEDT
Start	1224216779.827	04:13:00.827	15:13:00.827
End	1224216962.271	04:16:02.271	15:16:02.271
Duration	182.444 seconds		

Dataset name: 37-DynamicDayDamDust2

	Unix	UTC	AEDT
Start	1224217352.224	04:22:32.224	15:22:32.224
End	1224217563.883	04:26:04.883	15:26:04.883
Duration	211.659 seconds		

38 - Smoke

This dataset was acquired during daytime. An assistant held a smoke bomb. He tried to stay in a position where the smoke went towards the vehicle, therefore they needed to move a little. The figure 3.16 shows a photo of the situation. The photo was taken by the assistant holding the smoke bomb.

Dataset name: 38-DynamicDayDamSmoke

	Unix	UTC	AEDT
Start	1224217939.781	04:32:20.781	15:32:20.781
End	1224218021.286	04:33:41.286	15:33:41.286
Duration	81.505 seconds		

39 - Rain

This dataset was acquired at daytime. An assistant created a “water curtain” in front of the vehicle with a hose spraying water. Again, the assistant needed to move in order to keep the water in front of the vehicle. The figure 3.17 shows a photo of the situation.

Dataset name: 39-DynamicDayDamRain

	Unix	UTC	AEDT
Start	1224229665.084	07:47:45.084	18:47:45.084
End	1224229783.877	07:49:44.877	18:49:44.877
Duration	118.793 seconds		

Figure 3.15: Dynamic test around the lake with dust (Datasets 36 to 37)

Figure 3.16: Dynamic test around the lake with smoke (Dataset 38)

Figure 3.17: Dynamic test around the lake with simulated rain (Dataset 39)

40 - Clear, sun low in the sky

The dataset was acquired in the evening, just before the sunset. In this dataset there were no artificially created environmental conditions and no people moving.

Dataset name: 40-DynamicDayDamClear-SunLow

	Unix	UTC	AEDT
Start	1224230071.163	07:54:31.163	18:54:31.163
End	1224230243.984	07:57:24.984	18:57:24.984
Duration	172.821 seconds		

Summary

The following table summarizes the conditions for each of these datasets taken in this area with trees and lake.

Dataset	Dust	Smoke	Rain	Comment
35				Clear
36-37	X			
38		X		
39			X	
40				Sun low

3.3.4 Summary of *Dynamic* Datasets

The following table shows a summary of all conditions covered in all *dynamic* datasets. It does not precise the area in which the dataset was taken though, this precision can be found directly in the appropriate section. The default configuration is at daytime (i.e. the **Night** is only precised where appropriate).

Dataset	Dust	Smoke	Rain	Human	Night	Comment
25 to 28					X	Clear, at night
29 & 32						Clear
30 & 31	X					
33						Clear, Houses area
34				X		Houses area
35						Clear
36 & 37	X					
38		X				
39			X			
40						Clear

3.4 Calibration Datasets

3.4.1 Cameras

The data used to realize the calibrations concerning the Visual camera and the IR camera can be found respectively in the directories `VisualCameraCalibration` and `IRcameraCalibration`, which are both organised as follow. They contain the following directories:

- `LaserHorizontal`
- `LaserPort`
- `LaserStarboard`
- `LaserVertical`
- `VideoVisual` or `VideoIR` as appropriate

which content is as described for the previous datasets (see section 2.2).

In an additional directory, named `Calibration`, the following files and directories can be found:

- `Calib_Results.m` and `Calib_Results.mat` are the files exported by the Matlab Calibration Toolbox, contains all the calibration parameters estimated.
- `Images` is a directory containing the images that were used for the camera calibration process, named with successive numbers starting by 1, for convenience when loading them in Matlab.
- `matlabAsciiLaserData` is a directory containing the ascii descriptions of all laser data in files formatted to be suitable for Matlab, for convenience.

- `VideoLogAsciiCalibration.txt` is a text file figuring the timestamps for all images in `Images`, the number of line in this file corresponding to the number of the image as it is named in `Images` (e.g. the timestamp corresponding to the image named `image002.bmp` can be found at the line number 2 of `VideoLogAsciiCalibration.txt`).

The images in these datasets show a chess board exposed with various orientations in space, and at various distances. Note that these chess boards *are different for the Visual camera and the IR camera*. The size of the Black and White squares of these chess board are the following:

- for the IR camera: 114.8mm on both sides.
- for the Visual camera: 74.9mm on the axis *left-right* as it can be seen in the images and 74.7mm on the axis corresponding to the direction *up-down*.

3.4.2 Range Sensors (Lasers and Radar)

The data used for the range sensors calibration can be found in the directory named:

`RangeSensorsCalibration`

It is organized exactly as the regular datasets that were presented before (except that it does not contain the directories `RadarSpectrum` and `Payload`). Data from all sensors were collected in the so-called *open area*, with four vertical poles standing on a flat ground. These special features of known geometry as well as the vertical wall of the shed and the flat part of the ground were used to extract relevant data for the calibration process.

Chapter 4

Preliminary Analysis

This chapter proposes in its first section a preliminary analysis of the performance of the sensors considered in this work. It will focus, as an illustrative example, on the case of the presence of dust or smoke. In the second section, we propose some ideas to tackle the issue of challenging environments when using sensors for obstacle detection or terrain modeling.

4.1 Case Study

Lasers are extremely affected by dust and smoke. More precisely, a cloud of dust or smoke is almost seen as an actual obstacle. Thus, a basic analysis of the data provided by them might lead to *false detection* of large obstacles. This is all the more true as the SICK lasers only provide the information concerning the *first* return [1].

The radar operates at mm wavelengths, which makes the size of dust and smoke particles relatively much smaller, giving radar waves more penetration. Consequently, it is much less affected by dust or smoke, except for a slight increase of the level of noise in the data, and lower reflectivities for the returns. The following figures illustrate that statement.

Figure 4.1 and 4.2 show all the range values returned by the *LaserHorizontal* and the radar respectively, for a static test in clear conditions (dataset 02). All scans made during the complete duration of the dataset collection are drawn in these figures. The angle range corresponds to what is perceived in the test area: the first and last notable feature on the left and right of the graph are respectively the left and right poles of the trial frame (objects named *origin* and 1 in the table in section 3.2). Note that the laser, providing much more precise (raw) range measurements than the radar, detects all the objects that are located in its field of view, while the radar detects only the main ones and provides noiser data.

Figure 4.3 shows the same measurements from the laser and radar in the presence of dust (dataset 05). We can see that dust generates random points in the laser scans, located between the vehicle and the actual position of the obstacle.

Figure 4.4 shows that the results are similar in the presence of smoke: the laser sees it as an obstacle whereas the radar data are not significantly affected.

On figure 4.5 we can have a preliminary view of the effect of rain. The laser data are actually not particularly affected, except for a few specific points, which might be due to reflection effects on wet objects surfaces. This case warrants further investigation.

[1] some other lasers also provide information about a possible additional return. This might at least lead to some suspicion on the features perceived with a significant difference between these two returns.

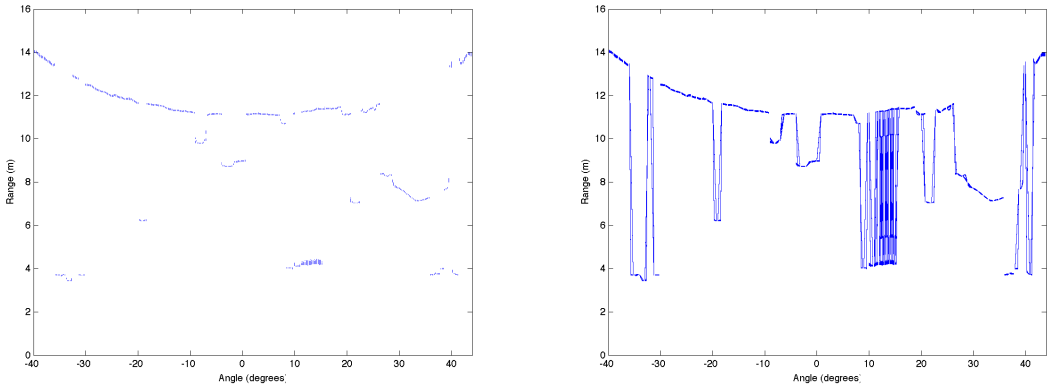

(a) Dots display (b) Lines display

Figure 4.1: Range returned by *LaserHorizontal* over angle, for static test in clear conditions (Dataset 02); displayed in dots in (a) and lines in (b)

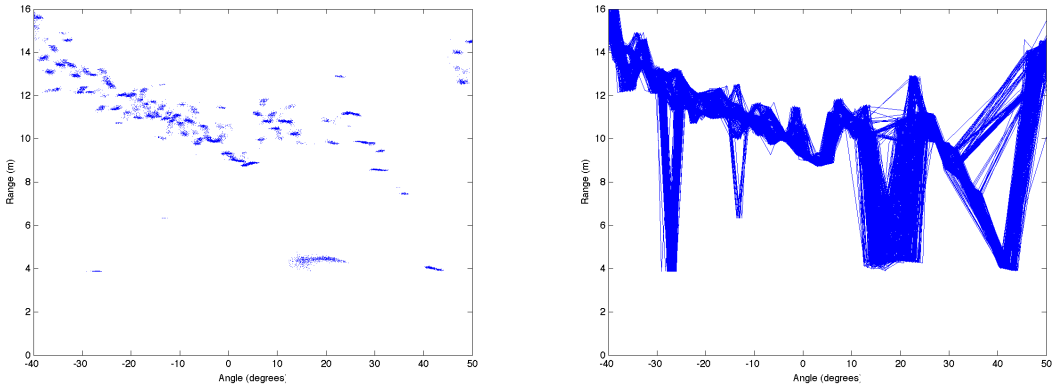

(a) Dots display (b) Lines display

Figure 4.2: Range returned by the radar (`RadarRangeBearing`) over angle, for static test in clear conditions (Dataset 02); displayed in dots in (a) and lines in (b)

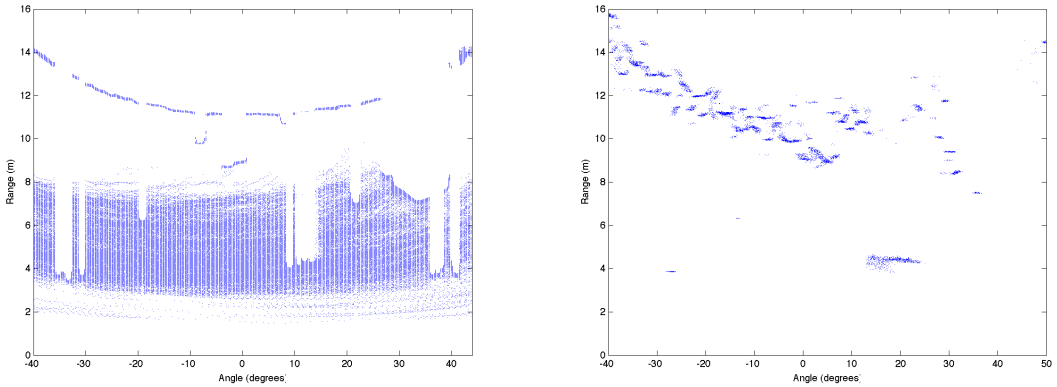

(a) LaserHorizontal (b) Radar

Figure 4.3: Range returned by the laserHorizontal and the radar (`RadarRangeBearing`) over angle, for static test with *heavy dust* (Dataset 05).

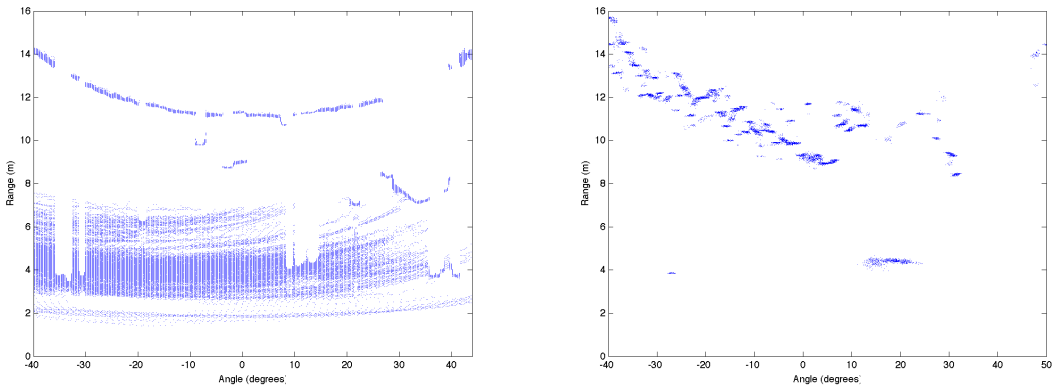

(a) LaserHorizontal (b) Radar

Figure 4.4: Range returned by the laserHorizontal and the radar over angle, for static test with *smoke* (Dataset 07).

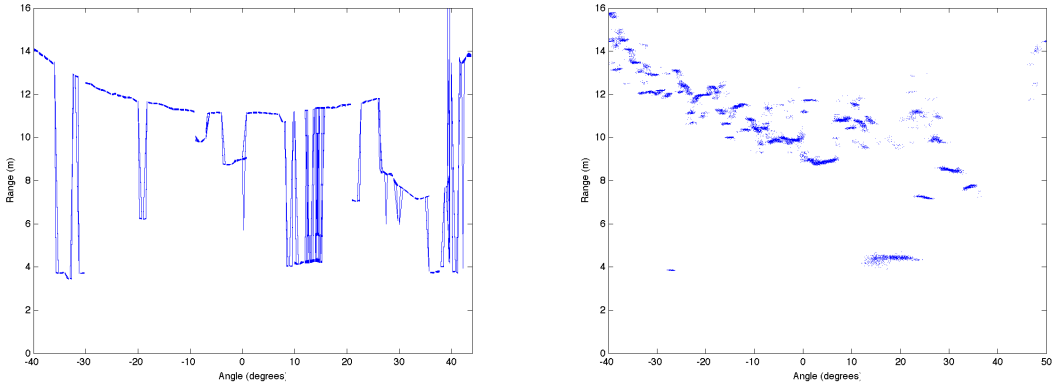

(a) LaserHorizontal (b) Radar

Figure 4.5: Range returned by the laserHorizontal and the radar over angle, for static test with *rain* (Dataset 08). The Laser data is here drawn with lines for an easier identification of the special reflection effects due to the presence of water on the objects (compare with figure 4.1 (b)).

Note that besides the lasers, both visual and thermal camera images are affected by dust (and smoke), but the effect is lower on the infra-red data, as infra-red waves have a higher penetration power.

4.2 Discussion

To avoid the problem of *false obstacles* created by conditions such as presence of dust or smoke, and increase the integrity of sensor data in general, one can benefit from the *redundancy* of sensors on a vehicle. This redundancy can be of different kinds. Let us consider a particular set of sensors.

- if these sensors are identical, i.e. they measure the same data (e.g. range) using the same process and the same physical characteristics (e.g. several 2D Sick Lasers), when their measurements overlap they may be directly compared to detect major failures only, such as a breakdown.
- if the sensors measure the same type of data (e.g. range), but in a different way (e.g. a laser scanner and a radar scanner, operating at different wavelengths), the comparison of their measurements may provide valuable information about the environment, to take an appropriate decision and be able to keep sensing abilities in an environment which is challenging for one type of sensor. For example: the radar waves penetrate dust and smoke much more easily than the laser ones, thus we know that in the presence of dust the radar will provide more accurate range measurement (it is the opposite in clear conditions).
- if the sensors measure different kinds of data (e.g a laser scanner and a colour camera), a comparison might still be made at a higher level of abstraction, for example after classification of pieces of the terrain in classes such as *obstacles* or *flat terrain*.

An example of the second case mentioned above is a preliminary study realized by James Underwood at ACFR to filter dust in range measurements provided by a laser and a radar. By comparing these measurements of the same area, knowing a model of the uncertainties involved, it is possible to identify when the error between data from these two sensors is too high, which means that the data should not be validated. In this study, as only two sensors are used, it is not possible to determine which one is wrong. Consequently, the only reasonable decision is to ignore both types of data (see figure 4.6). If an additional sensor, with different characteristics, is available, a more "informative" decision can be made if, for example, data from two sensors match while data from the third one shows a level of discrepancy.

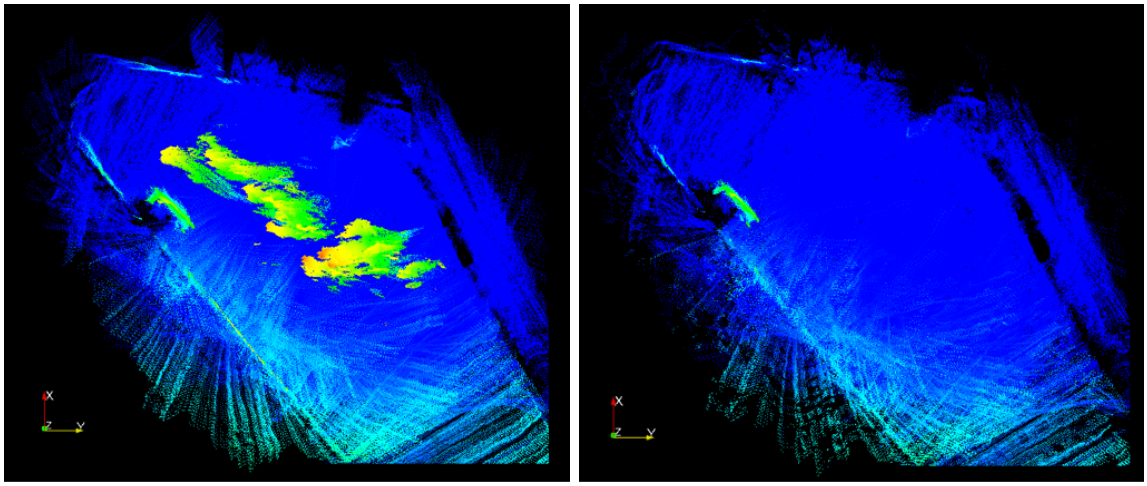

(a) Raw Laser Data (b) Filtered Laser Data

Figure 4.6: 3D points returned by a Laser Range Scanner during a dynamic test in presence of dust: before (a) and after (b) filtering. The green object visible in both images is a static car.

Acknowledgment

The authors of this document would like to thank Craig Rodgers, Marc Calleja, James Underwood, Andrew Hill and Tom Allen for their valuable contribution to this work.

Bibliography

[1] A. Alempijevic, S.R. Kodagoda, J.P. Underwood, S. Kumar, and G. Dissanayake. Mutual information based sensor registration and calibration. In *Procedings of the 2006 IEEE/RSJ Int. Conf. on Intelligent Robots and Systems*, 2006.

[2] Jean-Yves Bouguet. *Camera Calibration Toolbox for Matlab.* http://www.vision.caltech.edu/bouguetj/calib_doc/.

[3] Ross Hennessy. A generic architecture for scanning range sensors. Master's thesis, The University of Sydney, 2005.

[4] Andrea Monteriu, Prateek Asthan, Kimon Valavanis, and Sauro Longhi. Model-based sensor fault detection and isolation system for unmanned ground vehicles: Experimental validation (part ii). In *2007 IEEE International Conference on Robotics and Automation*, 2007.

[5] Andrea Monteriu, Prateek Asthan, Kimon Valavanis, and Sauro Longhi. Model-based sensor fault detection and isolation system for unmanned ground vehicles: Theoretical aspects (part i). In *2007 IEEE International Conference on Robotics and Automation*, 2007.

[6] T. Peynot and S. Lacroix. Selection and monitoring of navigation modes for an autonomous rover. In *10th International Symposium on Experimental Robotics 2006 (ISER '06)*, 2006.

[7] Robert Pless and Qilong Zhang. Extrinsic calibration of a camera and laser range finder. Technical report, Washington University in St. Louis, 2003.

[8] James Underwood, Andrew Hill, and Steven Scheding. Calibration of range sensor pose on mobile platforms. In *Procedings of the 2007 IEEE/RSJ Int. Conf. on Intelligent Robots and Systems*, 2007.

Australian Centre for Field Robotics
Rose Street Building J04
The University of Sydney NSW 2006 Australia
P **+61 2 9351 7126** F **+61 2 9351 7126** E **info@cas.edu.au** www.cas.edu.au

ARC Centre of Excellence for Autonomous Systems is a partnership between
AUSTRALIAN CENTRE FOR FIELD ROBOTICS | **The University of Sydney**
ARTIFICIAL INTELLIGENCE GROUP | **The University of New South Wales**
MECHATRONICS AND INTELLIGENT SYSTEMS GROUP | **University of Technology, Sydney**